

MASIM: An Efficient Multi-Array Scheduler for In-Memory SIMD Computation

Xingyue Qian¹, Chen Nie², Zhezhi He^{2,*}, and Weikang Qian^{1,3,*}

¹University of Michigan-SJTU Joint Institute, ²School of Electronic Information and Electrical Engineering, and ³MoE Key Lab of AI, Shanghai Jiao Tong University, Shanghai, China
Emails: {qianxingyue, chen.nie, zhezhi.he, qianwk}@sjtu.edu.cn; *corresponding authors

Abstract—Single instruction, multiple data (SIMD) is a popular design style of in-memory computing (IMC) architectures, which enables memory arrays to perform logic operations to achieve low energy consumption and high parallelism. To implement a target function on the data stored in memory, the function is first transformed into a netlist of the supported logic operations through logic synthesis. Then, the scheduler transforms the netlist into the instruction sequence given to the architecture. An instruction is either computing a logic operation in the netlist or copying the data from one array to another. Most existing schedulers focus on optimizing the execution sequence of the operations to minimize the number of memory rows needed, neglecting the energy-consuming copy instructions, which cannot be avoided when working with arrays with limited sizes. In this work, our goal is to reduce the number of copy instructions to decrease overall energy consumption. We propose MASIM, a multi-array scheduler for in-memory SIMD computation. It consists of a priority-driven scheduling algorithm and an iterative improvement process. Compared to the best state-of-the-art scheduler, MASIM reduces the number of copy instructions by 63.2% on average, which leads to a 28.0% reduction in energy.

I. INTRODUCTION

Traditional von Neumann architecture consists of a memory for data storage and a processor for data processing. It is the foundation of most modern computing systems, but it suffers from a problem called the *memory wall*: the energy spent on data transfer can be orders of magnitude larger than that on computation [1]. To break the wall, many *in-memory computing (IMC)* architectures have been proposed to enable memory arrays to perform logic operations such as XOR and majority (MAJ) so that costly data transfer can be reduced [2]–[4]. *Single instruction, multiple data (SIMD)* is a prevalent design style of IMC architectures with high parallelism [3]–[5]. In SIMD IMC, the calculation of the target function, *e.g.*, multiplication, on one input pattern is performed within a single column, and different columns are used to calculate the same function on different input patterns in parallel.

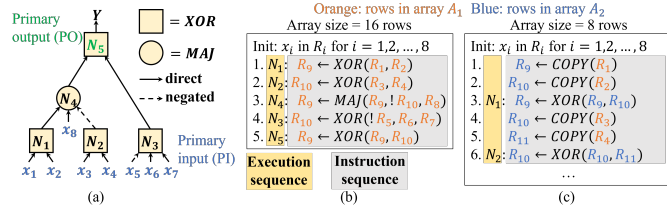


Fig. 1. An example of (a) a netlist, (b) an instruction sequence using a single array, and (c) an instruction sequence using multiple arrays.

To implement a target function on the SIMD IMC architecture, the function is first transformed into a netlist by a logic synthesis tool. A netlist example is shown in Fig. 1(a), in which each node corresponds to a supported logic operation. Then, a scheduler transforms the netlist into an *instruction sequence (IS)* that instructs the architecture to implement the function. An example of an IS is shown in the grey box in Fig. 1(c). In SIMD setup, an instruction is given to the rows of the memory arrays, and it is either performing a logic operation in the netlist or copying a row of an array to a row of another array. For example, in Fig. 1(c), the instruction $R_9 \leftarrow XOR(R_9, R_{10})$ is

an example of the former, which performs the XOR operation N_1 , while the instruction $R_9 \leftarrow COPY(R_1)$ is an example of the latter, which copies fanin x_1 from R_1 in array A_1 to R_9 in array A_2 . In what follows, we will also refer to performing a logic operation in the netlist as *computing a node* in the netlist.

Ideally, we want to use a single array to calculate the function as shown in Fig. 1(b), where each instruction in the IS computes a node in the netlist. In this case, most existing schedulers aim to reduce the number of rows needed during the calculation so that we can implement larger netlists within a single array with limited rows [4], [6]–[10]. These schedulers focus on optimizing the *execution sequence (ES)* of the nodes. An example of an ES of the nodes is the sequence of nodes N_1, N_2, N_4, N_3, N_5 shown in the yellow box of Fig. 1(b). For simplicity, in what follows, we refer to an ES of the nodes as an *ES*. We can see from Fig. 1(b) that to generate the IS corresponding to a given ES, we need to select a row for each node to store its result in. We call the process that generates the corresponding IS given an ES the *instruction generation (IG) process*. The IG process that minimizes the number of rows needed can be easily achieved by generating one instruction for each node to compute it and store its result in the available row with the smallest index [10].

However, when the number of needed rows exceeds the size of the array, we have to use multiple arrays as shown in Fig. 1(c). For SIMD IMC, a computation instruction can only be applied to the rows within the same array [4]. Thus, we need to insert copy instructions to copy the data from one array to another. However, a copy instruction is very energy-consuming: its energy consumption is 1.87 times that of a computation instruction [4]. Thus, the insertion of copy instructions can diminish the benefits offered by SIMD IMC [4], [8], [11].

Hence, it is important to reduce the number of copy instructions. However, existing schedulers do not take copy instructions into account when determining the ES. Given an ES, they use a naive [4] or greedy approach [10] to obtain the corresponding IS in the IG

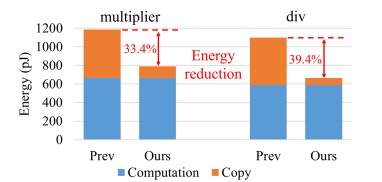


Fig. 2. Two examples of energy consumption of the same function implemented using the best prior method and our proposed method.

the row to store the result of each node, but also inserts necessary copy instruction before computing the node. In consequence, the resulting IS cannot minimize the number of copy instructions, and much energy is spent on copying data between the arrays. As shown in Fig. 2, in our experiment on two frequently used functions, multiplication and division, the energy spent on copying is almost as large as that spent on computation using the best scheduling result from the previous works [4], [8]–[10].

To address the above issue, this work proposes MASIM, a multi-array scheduler for in-memory SIMD computation, which aims at reducing the number of copy instructions given an array size limit. By reducing the number of copy instructions, the overall energy can be significantly reduced as shown in Fig. 2. Our main contributions

are as follows.

- We define a metric called the number of close partner pairs (CPPs), which can give a hint on the number of copy instructions needed in the future to help the scheduler make more judicious decision. We further propose a priority called CICPP, which combines the number of copy instructions and the number of CPPs (see Section III-B1). It serves as a key metric in MASIM.
- With CICPP, we propose a CICPP-driven scheduling algorithm, which can efficiently determine the ES while taking reducing copy instruction number into consideration, and the IS is also obtained during the process (see Section III-B).
- To further reduce the copy instruction number, we propose an iterative improvement process, which randomly perturbs the ES and then obtains the updated IS with a CICPP-driven IG strategy, which also exploits the CICPP priority (see Section III-C).
- We also make the code of MASIM open-source at <https://github.com/SJTU-ECTL/MASIM>.

The experimental results show that MASIM reduces the copy instruction number by 63.2% on average compared to the best existing scheduler, which leads to a 28.0% reduction in energy.

II. BACKGROUND

A. SIMD IMC

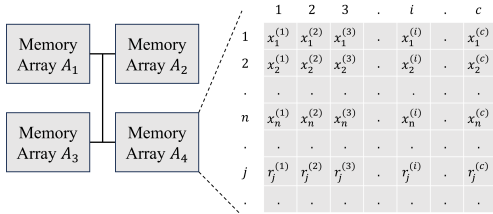


Fig. 3. Data layout in memory arrays.

SIMD is a popular IMC design style with high parallelism. Fig. 3 shows the data layout in a memory array with r rows and c columns. In the SIMD setup, the array can calculate the same function f on c different input patterns $X^{(1)}, \dots, X^{(c)}$ in parallel, where $X^{(i)} = (x_1^{(i)}, \dots, x_n^{(i)})$ is the i -th n -bit input pattern, and the i -th output pattern $Y^{(i)}$, where $Y^{(i)} = f(X^{(i)})$, is calculated in column i . Initially, the n -bit input pattern $X^{(i)} = (x_1^{(i)}, \dots, x_n^{(i)})$ is placed in the topmost n rows of column i as shown in Fig. 3. Then, the function is calculated by passing a sequence of instructions to the hardware as shown in Figs. 1(b) and 1(c). The instructions are given to the rows of the arrays, and the data stored in different columns of the same row are processed bitwise in parallel. For example, by passing the instruction $R_j \leftarrow XOR(R_1, R_2)$ to the array in Fig. 3, $r_j^{(i)} = XOR(x_1^{(i)}, x_2^{(i)})$ is computed for each $i = 1, \dots, c$.

However, an operation, *e.g.*, XOR and MAJ , can only be applied to the rows within the same array, whose size is limited [12]. In the example in Fig. 1(c), we assume that the arrays only have 8 rows. We cannot pass the instruction $R_9 \leftarrow XOR(R_1, R_2)$ to the hardware directly since the rows R_1 and R_2 are in array A_1 , while the row R_9 is in array A_2 . Instead, we need to insert copy instructions to copy the data in R_1 and R_2 to array A_2 before computing the operation in array A_2 (see instructions like $R_9 \leftarrow COPY(R_1)$ in Fig. 1(c)).

B. Netlist Representation and Scheduling Rules of SIMD IMC

As mentioned before, to fully exploit the potential of the SIMD IMC architecture, a scheduler is needed to automatically transform the netlist of the target function synthesized by the logic synthesis tool to the IS given to the hardware. In this work, we use XMG-GPPIC proposed in [4], which supports 3-input XOR and MAJ operation with fused negation, as the target hardware. Therefore, the corresponding netlist is an XOR -majority graph (XMG). However,

note that our method can be applied to other hardware with some minor modifications. Next, we explain the component of the XMG together with the scheduling rules using the XMG shown in Fig. 1(a).

- The primary inputs (PIs), which are shown in blue in Fig. 1(a), are initially stored in the topmost rows of the array. That is, the input x_i is stored in row R_i for $i = 1, 2, \dots, 8$. Since the PIs may be needed in the future when calculating other functions, they cannot be overwritten during the process.
- Each node in the netlist corresponds to a supported logic operation, *i.e.*, either a 3-input XOR or a 3-input MAJ . Note that in the figure, some operations only have 2 inputs, since the missing input is a constant 0 or 1, which is omitted for simplicity. In the SIMD setup, the operations are computed sequentially, and it takes one clock cycle to compute an operation.
- The directed edges indicate the dependency relation. If there is a directed edge from node i to node j , then the output of node i is the input of node j . If the edge is dashed, the output of node i is negated when it serves as the input of node j . We call node i a *fanin* of node j and node j a *fanout* of node i . A node can be computed in an array if and only if all its fanins are stored in that array. Furthermore, the hardware allows the output of a node to overwrite one of its inputs.
- The results of the primary outputs (POs), which are shown in green in Fig. 1(a), must be stored in the array when the schedule ends. However, the results of the other nodes can be overwritten when not needed any more.

C. Existing Schedulers

Many schedulers have been proposed for SIMD IMC architectures. Most of them focus on the computation within a single array. They aim to reduce the number of rows needed during the computation so that we can implement larger netlists within a single array with a limited size [6]–[10]. In order to achieve this, their main effort is to determine the ES. Given an ES, in order to use fewest rows, the row to store the computation result of each node can be simply selected as the available row with the smallest index [10]. The corresponding IS can be easily determined by computing one node per clock cycle according to the ES and storing its result in the chosen row without the need of copy instructions.

To determine the ES with the fewest rows needed, many methods have been proposed. OptiSIMPLER can obtain the ES with the optimal row requirement for the given netlist by formulating a Boolean satisfiability (SAT) problem [6]. However, since SAT solving is time-consuming, the scheduler can only be applied to small netlists. To support large netlists, other schedulers turn to heuristic approaches. Some schedulers are based on priority-driven scheduling. At each clock cycle, a node that is ready to be computed is picked according to a priority. The priority in the scheduler in [4] is adapted from that in [7], where a node that can remove more fanins from memory after scheduling it is favored. In STAR [9], the priority of a node n is determined by the minimum number of nodes that need to be computed before node n can be removed from memory. SIMPLER [8] performs a depth-first search on the netlist from the outputs until reaching a node that is ready to be computed. The traversal order of the fanins is determined by an optimistic estimation of the number of rows needed to calculate the fanins, *i.e.*, Strahler number [13]. Another recent work uses a divide-and-conquer approach that partitions a large netlist into small sub-netlists that can be scheduled by an optimal scheduler [10]. The scheduler outperforms previous ones in reducing the number of rows needed at the cost of a longer runtime since the solvers [14], [15] used in the scheduler are time-consuming.

Some existing schedulers also report their experimental results in terms of energy and delay when using multiple arrays [4], [10]. However, they do not make much effort to reduce the number of

copy instructions, so the resulting IS spends much energy in copying as shown in Fig. 2. Based on the obtained ES, XMG-GPPIC uses a naive IG strategy to select the row to store the result of each node and inserts necessary copy instruction [4]. Specifically, the array with the smallest index that contains enough available rows is selected to compute each node according to the ES. Before issuing the computation instruction, copy instructions are inserted to copy each fanin that is not stored in the selected array to an available row in the array. The recent work improves the naive strategy to a greedy one [10]. The array used to compute a node is selected so that the number of copy instructions inserted to copy its fanins is minimized. However, since the ES is determined to minimize the number of rows needed instead of the number of copy instructions, the result can still be much improved.

III. METHOD

A. Overview

As mentioned in Section II-B, a scheduler transforms the netlist of the target function into the IS given to the hardware. The instructions are executed by the hardware in serial with one instruction per clock cycle. Hence, the total energy for implementing the target function is the accumulation of the energy used to execute each instruction. To minimize the energy, we typically only allow computing each node (*i.e.*, performing the corresponding logic operation) in the netlist *once*. Thus, the total energy spent on executing all the computation instructions is fixed for a given netlist. Therefore, to minimize the total energy consumption, it is important to *minimize the total energy spent on executing all copy instructions*. In this work, we assume that the energy consumption of a copy instruction is constant. Thus, our target reduces to *minimize the number of copy instructions for a given netlist and a given array size*.

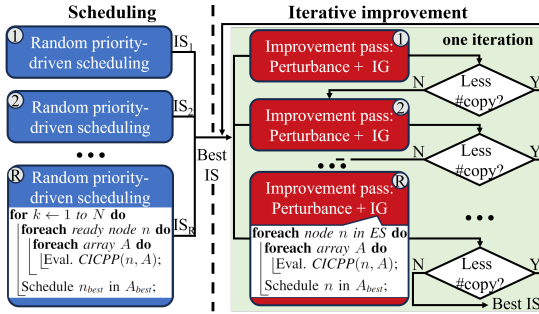


Fig. 4. The overall flow of MASIM.

Our proposed solution, MASIM, takes minimizing the copy instruction number into account when determining the IS. Its overall flow is shown in Fig. 4, which consists of two main parts, *i.e.*, a random priority-driven scheduling algorithm and an iterative improvement process.

In the first part, our scheduling algorithm needs to make the following three decisions iteratively until all nodes are scheduled: 1) **node choice**, *i.e.*, which node to be scheduled next, 2) **array choice**, *i.e.*, which array to schedule the node in, and 3) **row choice**, *i.e.*, which rows in the array are used to store the missing fanins and the result of the node. We call the missing fanins and the result of the node *incoming data*. We say a fanin i of n is *missing* in array A if i is not stored in array A . In MASIM, we use a metric called CICPP, which will be introduced in Section III-B1, as the priority when making these decisions. Once we have made the decisions, we generate the instructions to copy the missing fanins and then compute the chosen node accordingly. When there is a tie in priority, the scheduler picks a random choice. Hence, we call the scheduler *random CICPP-driven scheduler*. As shown in Fig. 4, the random scheduler is run for R times with different random seeds used in

breaking the ties to obtain the best IS, *i.e.*, the one with the minimum number of copy instructions. The details of the scheduling algorithm will be introduced in Section III-B.

In the second part, we attempt to iteratively improve the result. One iteration of this iterative process is shown in the green box in Fig. 4. In each iteration, we attempt to decrease the copy instruction number with at most R *improvement passes*, each shown as a red box. In each improvement pass, we first randomly perturb the ES in the best IS obtained so far. Then, we apply an IG process based on the new ES using the same CICPP priority. Note that the IG process only needs to make the last two decisions of the scheduling decisions, *i.e.*, array choice and row choice, since the node choice is decided by the given ES. If the resulting IS has fewer copy instructions, we accept it as *the best IS obtained so far* and begin a new iteration of the iterative improvement process. Otherwise, we begin another improvement pass in the current iteration. If none of the results in R improvement passes in an iteration is accepted, we end the flow and output the updated IS. The details of the improvement pass will be described in Section III-C.

B. Random CICPP-Driven Scheduling Algorithm

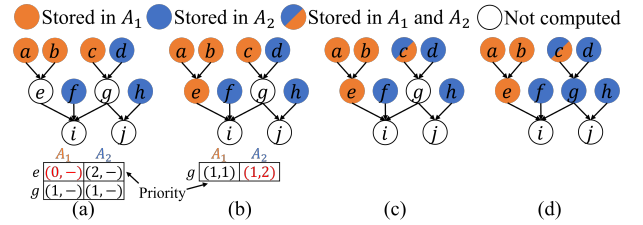


Fig. 5. Scheduling example: (a) the initial state of an outermost iteration of the random priority-driven scheduling; (b) compute e in A_1 ; (c) copy c to A_2 ; (d) compute g in A_2 .

The foundation of our scheduling algorithm is a priority-driven scheduler. We say that a node is *ready* if and only if all its fanins have already been computed and thus stored in the arrays. The overview of our scheduling algorithm is shown in the blue box at the bottom-left corner of Fig. 4. The outermost loop has N iterations, where N is the number of nodes in the given netlist. Each iteration of it decides the node choice, the array choice, and the row choice. Thus, after the loop finishes, all N nodes have been scheduled. To make the above three decisions in each iteration, we traverse each ready node n and each array A and evaluate the CICPP priority of scheduling n in A , denoted as $CICPP(n, A)$. Note that the corresponding row choice can be also obtained in the evaluation process to be illustrated in Section III-B2. Based on the evaluation results, we choose to schedule node n_{best} in array A_{best} with the highest $CICPP(n_{best}, A_{best})$ according to the corresponding row choice. That is, we copy the missing fanins of n_{best} to the selected rows and then compute n_{best} , putting its result in another selected row.

Example 1 Consider an example in Fig. 5(a). We want to decide the node and array choices for the next iteration. In the current state shown in Fig. 5(a), nodes e and g are ready since the fanins of e , *i.e.*, nodes a and b , and the fanins of g , *i.e.*, nodes c and d , have been computed and are stored in the arrays. We assume that the hardware has two arrays, A_1 and A_2 . We evaluate the priority of scheduling each ready node (*i.e.*, e and g) in each array (*i.e.*, A_1 and A_2). The evaluated priority is shown in the table in the figure. Among four possible choices, we choose to schedule node e in array A_1 , which gives the highest priority marked in red. The definition of the priority and the detailed values of the priorities in the table will be shown later.

In the following, we will first assume that the arrays have enough *empty rows* that contain no data so that we do not need to make the

row choice since we can use arbitrary rows to store the incoming data. Based on this assumption, we will explain the basic idea of CICPP priority in Section III-B1. Then, in Section III-B2, we will illustrate how to evaluate CICPP priority when taking the row choice into account.

1) *Basic Idea of CICPP Priority:* In this section, we introduce the basic idea of our CICPP priority under the assumption that the arrays have enough empty rows. We set minimizing the number of copy instructions needed to schedule the current node as our primary priority since it is the target of our scheduler.

Example 2 In the example in Fig. 5(a), among the four possible choices, scheduling node e in array A_1 does not need any copy instruction, while the other choices need 1 or 2 copy instructions. Thus, we decide to schedule e in array A_1 by generating a computation instruction, and the status of the nodes after this step is shown in Fig. 5(b). Note that in this case, the primary priority is enough to make the scheduling decision, so the secondary priority to be introduced below does not matter, and hence, it is denoted as “-” in the table in Fig. 5(a).

When there is a tie in the primary priority, we turn to our secondary priority. Before introducing it, we first give a few definitions. We say that node n and node i are *partners* of each other if they share a fanout x that has not been computed yet. If two partner nodes are stored in the same array A , we say that they form a *close partner pair* (CPP) in array A . In the example in Fig. 5(a), node a and node b form a CPP in array A_1 . Although node c and node d are partners of each other, they do not form a CPP since they are stored in different arrays. We propose to maximize the change in the number of CPPs, denoted as $\Delta\#CPP$, as our secondary priority. By maximizing $\Delta\#CPP$ in each step, we can reach a memory status with more CPPs, which is favorable since the fanins of a node to be scheduled are more likely to be stored in the same array, thus requiring fewer copy instructions in the future, as shown in the following example.

Example 3 In the example in Fig. 5(b), only node g is ready, and scheduling it either in array A_1 or in array A_2 needs one copy instruction, so we need to use the secondary priority. If we schedule g in A_1 , $\Delta\#CPP = 1$ since node g and node e form a CPP in A_1 . If we schedule g in A_2 , $\Delta\#CPP = 2$ since node g forms one CPP with node f and one with node h in A_2 . Therefore, we choose to schedule g in A_2 since it has a larger $\Delta\#CPP$ and potentially needs fewer copy instructions in the future. Given this choice, we first copy the missing fanin c into array A_2 (see Fig. 5(c)) and then compute g in A_2 (see Fig. 5(d)). Starting from the memory status in Fig. 5(d), we need one copy instruction to compute node i and node j , i.e., copying node e to array A_2 . However, if we schedule g in A_1 , we will need two copy instructions. This observation confirms the rationality of our secondary priority.

2) *Evaluation of CICPP Priority:* In this section, we illustrate the way to evaluate the CICPP priority to schedule node n in array A when taking the row choice into account. Since the rows we select will be used to store the incoming data, the original nodes stored in any of these rows will be overwritten, possibly leading to a reduction in the CPP number and hence, a negative $\Delta\#CPP$.

To facilitate our discussion, we use $N_{PA}(x, A)$ to denote the number of partners of node x stored in array A . By definition, when node x emerges in array A by copying or computing, the number of CPPs increases by $N_{PA}(x, A)$. When node x is overwritten in array A , the number of CPPs decreases by $N_{PA}(x, A)$.

As mentioned in Section III-A, to schedule node n in array A , we should first copy all the missing fanins to A . For each missing fanin i , we select a row in A and copy i to that row. Note that it is possible that the selected row cannot be directly overwritten, which requires some additional copy instructions that may change the

number of CPPs, which we will elaborate in Section III-B3. Thus, the selection of a row to store the missing fanin i will introduce some copy instructions and a change in CPP number. Suppose that the selection process needs $\#CI_i$ copy instructions and the change in CPP number is $\Delta\#CPP_i$. After the row is selected, we copy i to the row, which needs 1 copy instruction and increases the CPP number by $N_{PA}(i, A)$. Then, with all fanins stored in A , we compute n in A . We select a row in A to store the result of n . Suppose that the selection process needs $\#CI_n$ copy instructions and the change in CPP number is $\Delta\#CPP_n$. When computing n and storing its result in the selected row, we need 0 copy instruction, and the CPP number increases by $N_{PA}(n, A)$. Throughout this process, the two priorities are accumulated. That is, the total number of copy instruction needed, which is the primary priority for scheduling node n in array A , is $\sum_i(\#CI_i + 1) + \#CI_n$, and the total change in CPP number, which is the secondary priority for scheduling node n in array A , is $\sum_i(\Delta\#CPP_i + N_{PA}(i, A)) + \Delta\#CPP_n + N_{PA}(n, A)$.

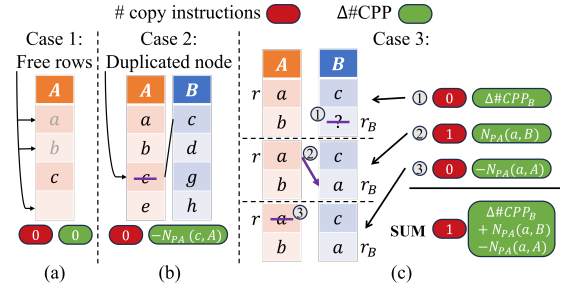


Fig. 6. Row selection strategy: (a) Case 1; (b) Case 2; (c) Case 3.

3) *Row Selection Strategy:* Now we illustrate our row selection strategy using Fig. 6. In the figure, the number of copy instructions is shown in the red circles and $\Delta\#CPP$ is shown in the green circles. As mentioned in Section III-B2, the number of copy instructions and $\Delta\#CPP$ for a row selection will be accumulated in the total CICPP priority, so the row selection is also done according to CICPP priority, i.e., we attempt to minimize the number of copy instructions and maximize $\Delta\#CPP$. When we need to select a row in array A , the array belongs to one of the following three cases with decreasing priority. We illustrate our strategy for each case.

Case 1 is the ideal case where there are free rows in the array, as shown in Fig. 6(a). A row is said to be *free* if it is empty or the stored node is no longer needed. For example, in Fig. 5(b), after computing node e in array A_1 , the results of node a and node b are no longer needed and can be overwritten without any potential disadvantage, so we mark them in grey in Fig. 6(a), and the rows storing their results are regarded as free rows. In this case, we select an arbitrary free row, and no copy instruction is needed and $\Delta\#CPP = 0$.

In **Case 2**, there is no free row in the array, but there are duplicated nodes stored in the array as shown in Fig. 6(b). A node is said to be *duplicated* if 1) it is needed for the future computation, i.e., it is a PO or has fanouts that have not been computed yet, and 2) it is stored in more than one array. For example, in Fig. 5(c), node c is duplicated since it has a fanout g that has not been computed yet, and it is stored in both arrays A_1 and A_2 . Ideally, we avoid overwriting a duplicated node in an array, since we may need to compute its fanouts in that array. For example, if we overwrite node c in array A_2 with the computation result of another node before scheduling node g in Fig. 5(c), c will be missing when scheduling g , so extra copy instructions will be needed to compute g . However, when there is no free row in an array, we have to select a row that stores a duplicated node and overwrite it, which is indicated by the purple line in Fig. 6(b). When overwriting duplicated node c in array A , the number of CPPs is reduced by $N_{PA}(c, A)$, and among all duplicated nodes stored in array A , we choose to overwrite the one

with the minimum CPP number reduction. In this case, still no copy instruction is needed, but $\Delta\#CPP$ may be a negative number, which is less favorable.

Case 3 is the worst case where there is no free row and all nodes stored in the array A are not duplicated, as shown in Fig. 6(c). Since the nodes are not duplicated, but will still be needed in the future, we cannot simply overwrite them. Instead, if we want to select a row r in array A , we first need to insert a copy instruction to copy the node a stored in r to another array B . This raises a new question: which row in B should we use to store the copied a . We propose a three-step procedure to select a row r in A . In Step ①, as shown in Fig. 6(c), we select a row r_B in another array $B \neq A$ using the row selection strategy for Case 1 or 2. That is, we select a free row or a row containing a duplicated node in B . If no row can be selected in this way, we move on to the next available array. In Step ②, no copy instruction is needed and the change in CPP number is denoted as $\Delta\#CPP_B$. In Step ③, we generate a copy instruction to copy a from row r to row r_B as indicated by the purple arrow in Fig. 6(c). In this step, 1 copy instruction is needed and the change in CPP number is $N_{PA}(a, B)$. In Step ④, we overwrite node a in array A , which has become duplicated, as shown in Fig. 6(c). In this step, no copy instruction is needed and the change in CPP number is $-N_{PA}(a, A)$. In total, 1 copy instruction is needed and $\Delta\#CPP = \Delta\#CPP_B + N_{PA}(a, B) - N_{PA}(a, A)$. We traverse every node a stored in array A and every other array B . Among all possible choices, we pick node a_{best} and array B_{best} so that $\Delta\#CPP$ is maximized and the row r_{best} containing node a_{best} is our choice.

C. Improvement Pass

In this section, we describe the improvement pass. As mentioned in Section III-A, we first randomly perturb the ES and then apply the IG process given the new ES.

We first describe the random perturbation by an example in Fig. 7. Assume that the original ES is d, a, b, f, c, e . To perturb it, we first randomly pick a time step index, e.g., 2. At time step 2, node a is chosen to be scheduled in the original ES, as shown in Fig. 7. However, nodes $b, c,$ and f are also ready to be computed. Initially, they are not chosen because they have a lower priority than a , or they have the same priority as a , but they are not picked due to randomness. Since picking the node with the highest priority is just a heuristic that cannot always guarantee the best performance, we attempt to make a different node choice, hoping to improve the performance. Thus, we randomly pick another ready node, e.g., node c , and insert it right before a in the original ES, which leads to the new ES d, c, a, b, f, e as shown in Fig. 7.

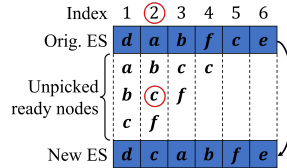


Fig. 7. An example of perturbing the execution sequence.

Given the new ES, we propose to apply a *CICPP-driven IG process* to generate the corresponding IS, which is shown in the red box in the bottom-right corner of Fig. 4. The process is similar to the scheduling algorithm in Section III-B. The difference lies in that in each outermost iteration i , instead of traversing both the ready nodes and the available arrays to choose the node and the array with the highest priority, we fix the node as the i -th node in the ES and only traverse the arrays to pick the one with the highest priority. For example, given the new ES in Fig. 7, we first schedule node d by inserting the copy instructions needed followed by the computation instruction for node d , then move on to node c , and so on.

IV. EXPERIMENTAL RESULTS

This section shows the experimental results. We implement MASIM and some prior state-of-the-art schedulers used for comparison in C++ and perform experiments on a computer with a 24-core 2.4GHz Intel 4214R processor and a 64GB RAM using 12 threads.

Our target is to develop a scheduler that can minimize the number of copy instructions needed for a given array size limit, thus reducing the overall energy consumption. Hence, the same netlist is given as input to all schedulers. We use Mockturtle [16] to synthesize the target functions into the XMGs supported in XMG-GPPIC [4]. Since it takes time and energy to compute each node in the netlist in serial, we attempt to minimize the size of the netlist, i.e., the number of nodes, in the synthesis step. For this purpose, we repeatedly apply the widely-used logic optimization command sequence *resyn2* from ABC [17] to the netlist until its size cannot be reduced any more.¹

Table I. Benchmarks used in the experiment.

Benchmark	#Nodes	PI	PO	Benchmark	#Nodes	PI	PO
int2float	199	11	7	max	1824	512	130
router	201	60	3	sin	3482	24	25
cavlc	600	10	11	sqrt	9240	128	64
priority	551	128	8	multiplier	14176	128	128
dec	304	8	256	div	12536	128	128
adder	256	129	256	log2	19760	32	32

The benchmarks used in our experiments are from the EPFL benchmark suite [18]. The information of the optimized netlist of each benchmark is listed in Table I. For some benchmarks, some of their POs are just the PIs or constant 0 or 1, so we do not include these POs into the netlists.

Balancing runtime and performance, we set the parameter R in Fig. 4 as 500. We use the same set of rules as described in Section II-B for all schedulers. For existing schedulers that do not allow the output of a node to overwrite one of its inputs, we adjust them slightly to permit such overwriting while still maintaining the core algorithms intact. The existing schedulers such as GPPIC [4], SIMPLER [8], and STAR [9] are relatively fast. For a fair comparison, we modify them to enhance their performance. Specifically, we add randomness to their methods. When there is a tie in priority, we pick a random node among the ones with the highest priority instead of the one with the smallest index. The improved existing schedulers are run for multiple times until they reach the same runtime as ours, and the best results are reported for each method. Note that to ensure performance improvement, we run the original scheduling algorithm as the first run in the improved version. The IG strategy used for the previous schedulers is the greedy strategy proposed in [10] since it gives better performance than the naive method proposed in [4].

We set a different array size limit for each benchmark according to the size of the netlist so that MASIM uses 2-4 arrays to implement the benchmark. The array size and the number of arrays used by MASIM for each benchmark are listed in columns 2 and 3 of Table II, respectively. The correctness of the scheduling results is verified by a simple algorithm. Next, in Section IV-A, we compare the number of copy instructions obtained by different schedulers. In Section IV-B, we compare the resulting energy consumption. In Section IV-C, we perform the ablation study. In Section IV-D, we study the performance of various schedulers when different array sizes are considered.

A. Performance on Reducing Copy Instruction Number

In Table II, columns 4–8 list the numbers of copy instructions obtained by the existing schedulers [4], [8]–[10], and MASIM, while columns 12 and 13 list their runtimes. For each benchmark, we highlight the best scheduling result, i.e., the one with the least number of copy instructions, in bold. We can see that MASIM achieves the fewest copy instructions among all methods for all benchmarks. Compared to XMG-GPPIC [4], SIMPLER [8] and STAR [9], it reduces the number of copy instructions by 75.2%, 73.2%, and 72.6%, respectively, on average using the same runtime. Compared

¹In our implementation, we use the Mockturtle version of *resyn2*.

Table II. Numbers of copy instructions obtained by various schedulers and their runtimes.

Benchmark	ArraySize	#Array	#Copy								Time(s)		
			[4]	[8]	[9]	[10]	MASIM	[10]+IG	NoImpr	[10]+Impr	[10]	[4], [8], [9], MASIM	NoImpr
int2float	16	2	252	220	222	<u>211</u>	87	105	114	179	43	6	3
router	64	2	188	170	169	<u>176</u>	70	88	71	152	19	9	7
cavlc	64	2	421	205	281	<u>54</u>	19	24	26	49	227	72	41
priority	128	2	<u>238</u>	<u>238</u>	<u>238</u>	<u>238</u>	128	128	128	238	235	30	20
dec	256	2	<u>18</u>	<u>20</u>	<u>18</u>	<u>18</u>	9	9	9	18	92	24	15
adder	256	2	<u>512</u>	<u>512</u>	<u>512</u>	<u>512</u>	256	256	256	512	42	29	21
max	256	4	<u>2294</u>	<u>1726</u>	<u>1725</u>	<u>1723</u>	937	1250	1156	1723	149	97	71
sin	256	2	687	1574	572	<u>423</u>	120	132	136	361	809	502	483
sqrt	256	3	4915	4639	4701	<u>4331</u>	1290	1307	1478	4039	1437	135	111
multiplier	256	2	16009	7303	11231	<u>5961</u>	1440	1736	1643	5525	1131	708	596
div	256	3	6144	6013	7609	<u>5812</u>	872	926	965	4986	1339	700	439
log2	256	4	11388	14702	12581	<u>7043</u>	3311	3878	3793	6414	2465	886	732
GEOMEAN			922.4	854.7	835.3	622.5	228.8	258.2	257.9	574.7	262.9	88.6	63.1

to the recent work [10], it reduces the number of copy instructions by 63.2% on average with only 33.7% of the runtime. Compared to the best result obtained by the existing schedulers [4], [8]–[10] for each benchmark, which is underlined in the table, MASIM still reduces the number of copy instructions by 63.1% on average. For two commonly-used large benchmarks, multiplier and divisor, MASIM only needs less than 1/4 and 1/6 copy instructions, respectively, compared to the best result. The results demonstrate the ability of MASIM in reducing the number of copy instructions.

B. Performance on Reducing Energy Consumption

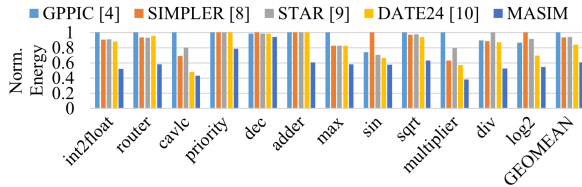


Fig. 8. Energy comparison.

In this section, we compare the energy consumption of the ISs obtained by different schedulers. To obtain the energy consumption of a given IS, we accumulate the energy consumption of each instruction. The energy consumption of each type of instruction, *i.e.*, computation instruction and copy instruction, for each array size is obtained using the method from [4]. For each benchmark, we normalize the energy to the maximum of the five methods. As shown in Fig. 8, compared to XMG-GPPIC [4], SIMPLER [8], STAR [9], and DATE24 [10], MASIM reduces the total energy consumption by 39.4%, 35.4%, 35.7%, and 28.0%, respectively, on average. Note that the energy reduction is less prominent than the copy instruction number reduction, since some portion of the energy is spent on computation instructions that cannot be saved. The results show the ability of MASIM in reducing energy consumption.

C. Ablation Study

There are two main parts in our schedulers: CICPP-driven scheduling algorithm that can determine the IS and the iterative improvement process that improves the obtained IS. In the iterative improvement process, the CICPP-driven IG strategy described in Section III-C, which generates the IS given the ES, is also an important component. We study the effect of each of them as follows.

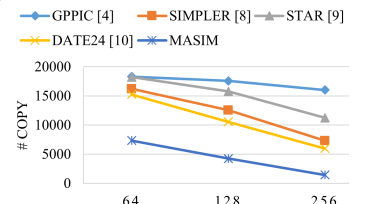
1) *CICPP-Driven IG*: In Table II, the column “[10]” lists the number of copy instructions obtained using the ES given by the scheduler in [10] and the greedy IG [10]. The column “[10]+IG” lists the number of copy instructions obtained using the same ES and our CICPP-driven IG. The results show that our CICPP-driven IG achieves fewer copy instructions for all benchmarks. On average, it reduces the number of copy instructions by 58.5%, showing the strength of our CICPP-driven IG. Note that both IG methods are very fast compared to the scheduling algorithms, so we do not compare their runtimes.

2) *CICPP-Driven Scheduling Algorithm*: In Table II, the column “NoImpr” lists the number of copy instructions obtained using our CICPP-driven scheduling algorithm without the following iterative improvement process, and its runtime is listed in the last column. Compared to the best existing scheduler [10], it reduces the number of copy instructions by 58.6%. Even compared to the enhanced version of [10] using the CICPP-driven IG, *i.e.*, “[10]+IG”, it achieves a bit fewer copy instructions by only using 24% of the runtime, showing the efficiency of our CICPP-driven scheduling algorithm.

3) *Iterative Improvement Process*: In Table II, the column “[10]+Impr” lists the number of copy instructions obtained based on the result of [10] and improved using our proposed iterative improvement process. Note that to make the comparison fair, the IG used in this version is the greedy IG used in [10]. Comparing “[10]+Impr” and “[10]”, the iterative improvement process reduces the number of copy instructions by 7.7%. Comparing MASIM and “NoImpr”, which are the MASIMs with and without the iterative improvement process, respectively, the iterative improvement process reduces the number of copy instructions by 11.3%. This shows the strength of our iterative improvement process.

D. The Impact of Different Array Sizes

In this section, we study the impact of different array sizes on the number of copy instructions needed to implement the benchmark *multiplier* for various schedulers. We consider three array sizes: 64, 128, and 256. The result is shown in Fig. 9. As expected, the number of copy instructions needed decreases with the array size, and MASIM outperforms the existing methods for all array sizes.

Fig. 9. Number of copy instructions needed for *multiplier* using different array sizes.

V. CONCLUSION

In this work, we propose MASIM, a multi-array scheduler for SIMD IMC, which can significantly reduce the number of energy-consuming copy instructions needed when multiple arrays are used in SIMD IMC. It involves a priority-driven scheduling algorithm that uses the number of copy instructions as the primary priority and the number of CPPs, which is a new metric we propose, as the secondary priority. To further reduce the copy instruction number, we propose an iterative improvement process. MASIM reduces the number of copy instructions by 63.2% on average compared to the best prior scheduler, leading to a 28.0% reduction in energy consumption. In this work, we assume that the energy consumption of a copy instruction is a constant. However, it generally takes less energy to copy data between arrays that are located close to each other on the chip. We will extend MASIM to handle this situation in the future.

REFERENCES

- [1] A. Pedram *et al.*, “Dark memory and accelerator-rich system optimization in the dark silicon era,” *IEEE Design & Test*, vol. 34, no. 2, pp. 39–50, 2017.
- [2] S. Kvatinsky *et al.*, “MAGIC–memristor-aided logic,” *IEEE Trans. Circuits Syst. II, Exp. Briefs*, vol. 61, no. 11, pp. 895–899, 2014.
- [3] N. Hajinazar *et al.*, “SIMDRAM: A framework for bit-serial SIMD processing using DRAM,” in *ASPLOS*, 2021, pp. 329–345.
- [4] C. Nie *et al.*, “XMG-GPPIC: Efficient and robust general-purpose processing-in-cache with XOR-Majority-Graph,” in *GLSVLSI*, 2023, pp. 183–187.
- [5] J. Wang *et al.*, “A 28-nm compute SRAM with bit-serial logic/arithmetic operations for programmable in-memory vector computing,” *IEEE J SOLID-STATE CIRCS*, vol. 55, no. 1, pp. 76–86, 2020.
- [6] D. Bhattacharjee *et al.*, “Synthesis and technology mapping for in-memory computing,” in *Emerging Computing: From Devices to Systems: Looking Beyond Moore and Von Neumann*, 2022, pp. 317–353.
- [7] M. Soeken *et al.*, “An MIG-based compiler for programmable logic-in-memory architectures,” in *DAC*, 2016, pp. 1–6.
- [8] R. Ben-Hur *et al.*, “SIMPLER MAGIC: Synthesis and mapping of in-memory logic executed in a single row to improve throughput,” *TCAD*, vol. 39, no. 10, pp. 2434–2447, 2020.
- [9] F. Wang *et al.*, “STAR: Synthesis of stateful logic in RRAM targeting high area utilization,” *TCAD*, vol. 40, no. 5, pp. 864–877, 2021.
- [10] X. Qian *et al.*, “An efficient logic operation scheduler for minimizing memory footprint of in-memory SIMD computation,” in *DATE*, 2024.
- [11] N. Talati *et al.*, “Practical challenges in delivering the promises of real processing-in-memory machines,” in *DATE*, 2018, pp. 1628–1633.
- [12] X. Dong *et al.*, “NVSim: A circuit-level performance, energy, and area model for emerging nonvolatile memory,” *TCAD*, vol. 31, no. 7, pp. 994–1007, 2012.
- [13] D. Auber, “Using Strahler numbers for real time visual exploration of huge graphs,” in *International Conference on Computer Vision and Graphics*, vol. 1, 2002, p. 3.
- [14] L. de Moura *et al.*, “Z3: An efficient SMT solver,” in *TACAS*, 2008, pp. 337–340.
- [15] L. Gurobi Optimization, “Gurobi optimizer reference manual,” 2021.
- [16] M. Soeken *et al.*, “The EPFL logic synthesis libraries,” 2022, arXiv:1805.05121v3.
- [17] B. Brayton *et al.*, “ABC: An academic industrial-strength verification tool,” in *Proceedings of the 22nd International Conference on Computer Aided Verification*, 2010, p. 24–40.
- [18] L. Amarù *et al.*, “The EPFL combinational benchmark suite,” in *IWLS*, 2015.